This paper reports a study of the electromagnetic processes in self-generating resonant inverters, as well as the derivation of analytical dependences of their operating frequency on the parameters of the resonance circuit and positive feedback circuits, in order to expand the range of their output power and optimize their operation. The object of research is electromagnetic processes in resonant inverters, in which autogeneration of resonant current oscillations is carried out in the process of operation. The results of studying the electromagnetic processes in sequential self-generating resonant inverters based on the characteristics of the resonant circuit are presented. The operating modes of the inverters have been optimized by setting certain ratios between the operating and resonant frequencies at unstable circuit parameters. The ratio of operating and resonant frequencies is set through the use of phase-shifting filters in a positive feedback loop along the circuit current and correspond to the autogenerator mode. The conditions of self-generation in converters with a sequential resonant circuit have been determined. Mathematical expressions have been built for determining the coefficients of positive feedback on the current and voltage of the resonant circuit, which made it possible to derive target analytical dependences. Analytical dependences of the established operating frequency on the parameters of the circuit and phase-shifting filters have been established. Based on the obtained dependences, the parameters of the positive feedback circuits have been determined in order to ensure a wide range of output power of the converters. The resulting dependences make it possible to carry out theoretical calculations whose results repeat the results of model experiments. Phase characteristics of the resonance circuit and various phase-shifting filters, which can be part of a serial resonant converter, have been constructed. The results of the analysis reported here could be used in the design of resonant inverters with unstable circuit parameters, in particular in inductive chargers

Keywords: *self-generating resonant inverter, operating frequency, Q factor of sequential resonance circuit, positive feedback*

UDC 621.314
DOI: 10.15587/1729-4061.2022.252148

OPTIMIZING THE OPERATION OF CHARGING SELF-GENERATING RESONANT INVERTERS

Gennadiy Pavlov
Doctor of Technical Sciences, Professor*
Andrey Obrubov
PhD, Associate Professor
Department of Ship Power Systems**
Irina Vinnichenko
Corresponding author
PhD, Associate Professor*
*Department of
Computerized Control Systems**
**Admiral Makarov National University
of Shipbuilding
Heroiv Ukrainy ave., 9, Mykolaiv, Ukraine, 54007

Received date 14.12.2021
Accepted date 30.01.2022
Published date 25.02.2022

How to Cite: *Pavlov, G., Obrubov, A., Vinnichenko, I. (2022). Optimizing the operation of charging self-generating resonant inverters. Eastern-European Journal of Enterprise Technologies, 1 (5 (115)), 23–34. doi: https://doi.org/10.15587/1729-4061.2022.252148*

1. Introduction

Chargers with contactless energy transmission are in demand in the transport industry and will be used on an even larger scale in the future [1]. They make it possible to recharge the traction batteries of the rolling stock of both ground [2] and water [1] autonomous electric vehicles without additional time spent on electrical connection and disconnection. It is known [1, 3] that non-contact chargers transmit energy mainly by inductive means; most of their designs include resonant inverters. Their power output varies from 1 kW [3] to 500 kW [2] depending on the capacity of the battery to be charged and the requirements for the charging speed. The phenomenon of electrical resonance solves, in this case, two problems: ensuring the soft switching of the power keys and compensating for the parasitic leakage inductances of the inductor coils. Therefore, research on the development and improvement of resonant inverters for non-contact chargers is relevant.

2. Literature review and problem statement

In transducing equipment, pulsed inverters with independent excitation of oscillations [4–7] have become widespread, in which a separate independent generator serves as the source of the inverter control signal. In study [4], to increase the power of resonant inverters, a dual power circuit with a packet control mode is used, which preserves optimal switching conditions. The impulse sequence is formed by the control system. Power adjustment is implemented by changing the number of pulses. However, to compensate for significantly changing circuit parameters, it is necessary to accurately monitor the phase of oscillations in the circuit. Paper [5] also uses a packet-pulse method of power regulation, which is effective with a relatively stable resonant circuit and provides optimal switching conditions in a wide range of regulation. A typical example of a system with independent excitation of oscillations is a chip of the UCC25600 type for the construction of an LLC-resonance converter [6], and similar ones, which have become widespread in power systems of consumer and industrial electronics. High efficiency and low generated interference in these converters are provided with integrated inductive elements. Frequency regulation compensates well for changes in load current but, if the resonance network becomes non-stationary, then additional feedback channels must be introduced into the control system to compensate for complex perturbations. This could adversely affect the stability of regulation.

Options for overcoming the problems of compensation of complex perturbations in a resonant converter system can be the combination of methods for regulating the power of converters. This approach is used in [7], where frequency regulation combined with switching the topology of the inverter circuit is used to adjust the power of the bidirectional converter system. However, the complication of the power circuit of the inverter and the control system is not always

acceptable for reasons of reliability under conditions of exposure to powerful electromagnetic interference.

In this sense, an alternative is autogenerator circuits of converters that maintain oscillations using signals of their own power circuit [8–10]. They have a significant advantage for resonant converters – the relationship of the operating frequency of self-generation with the parameters of the circuit and, as a result, the automatic change in the operating frequency and the maintenance of the mode of resonance compensation of unstable leakage inductances. In the process of non-contact charging, the leakage inductances change significantly when the mutual position of the charging inductors changes. Therefore, the principle of self-generation [8] is advisable to use in resonant inverters of inductive chargers.

Paper [9] shows that self-generation in the inverter is implemented due to positive feedback on the circuit current in an integrated transformer with an additional winding. The advantages of the scheme are improved controllability and self-adjustment with variations in load parameters. The implementation of these advantages in non-contact chargers requires the development of special circuit solutions that replace the integrated transformer, compatible with the inductor system. For example, work [10] implemented an original circuit solution of positive feedback with a separate low-power resonance system, which is similar in properties to the power resonance system. Owing to this separation, the stability of self-generation increases, but the self-adjustability of the inverter decreases when leakage inductances change in the power resonance system. Therefore, in non-contact chargers with self-generation in positive feedback, it is advisable to use phase-shifting non-resonant filters of the first or second order. The low steepness of the phase characteristic of these filters would contribute to the self-tuning of the inverter with variations in the leakage inductances of the resonance system.

Switching conditions are also an important aspect of charging inverters. With certain ratios of the conversion frequency and the resonant frequency of the circuit, it is possible to achieve the conditions of soft switching of power valves with low power losses and an increase in the amplitude of oscillations as a result of resonant phenomena in the circuit, as shown in [11, 12]. In [11], soft switching takes place at a constant operating frequency and a variable number of pulses; in [12], the achievement of soft switching conditions using switching keys is shown. In both cases, the operating frequency is related to the parameters of the power circuit. When any parameter of the power circuit changes, in order to maintain the conditions of soft switching of the keys, the operating frequency of the inverter must be adjusted accordingly. The above allows us to assert that studying the dependences of the operating frequency of the inverter with self-generation on the parameters of the resonant circuit is expedient for improving powerful non-contact chargers.

3. The aim and objectives of the study

The purpose of this work is to derive analytical dependences of the established operating frequency of resonant converters on the parameters of the circuit and positive feedback circuits characteristic of their autogenerator mode of operation and making it possible to expand the range of output power. This could help determine the parameters of positive feedback circuits in inverters with self-generation. The results of the study would make it possible to implement self-adjustment of the operating frequency of the non-contact charger when the inductance of the resonant circuit changes within wide limits.

To accomplish the aim, the following tasks have been set:

– to define the classification of methods of excitation of oscillations in the circuits of resonant inverters;

– to perform a comparative analysis of ways to implement self-generation in resonant inverters using non-resonant filters;

– to analyze the conditions of key switching;

– to determine the conditions for self-generation of oscillations and theoretical and experimental (obtained as a result of simulation modeling) dependences of the established frequency of self-generation on the parameters of the circuit and the positive feedback circuit;

– to conduct simulation modeling of the transformers under consideration to verify the results of theoretical research.

4. The study materials and methods

The study uses methods of differential and integral calculus, numerical methods for calculating analytical dependences, methods of simulation modeling of processes in the schemes of resonant inverters.

5. Results of studying self-generation conditions in serial resonant inverters

5. 1. Classification of methods of excitation of oscillations in the contours of resonant inverters

We next consider the methods of excitation of oscillations and their control: independent, self-generator, mixed, and synchronous (Fig. 1).

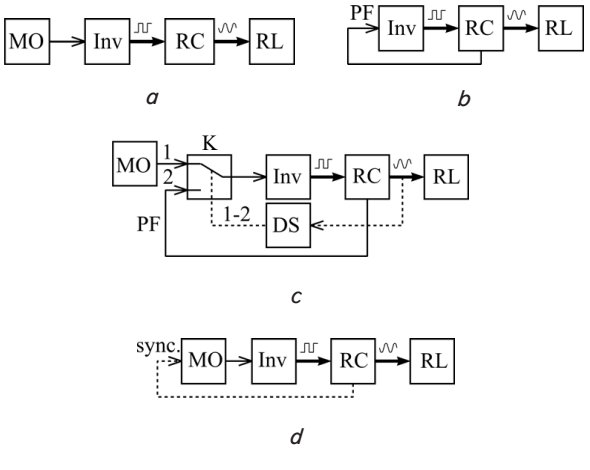

Fig. 1. Inverters with various methods of excitation of oscillations and their control: *a* — scheme of independent excitation of oscillations; *b* — scheme of self-generator excitation of oscillations; *c* — scheme of mixed excitation of oscillations; *d* — scheme of excitation of oscillations with synchronous control; MO – Master Oscillator; Inv – Inverter; RC – Resonant Contour; RL – Rectifier with load; PF – Positive Feedback; DS – Detector Sensor — the sensor-detector of the amplitude of oscillations in the circuit (the dotted line indicates the signal of temporary action); K — signal switch

Independent excitation of oscillations with asynchronous control (Fig. 1, *a*) is carried out using an autonomous controlled oscillation generator (MO), in which parameters such as frequency, duty cycle, number of pulses can be adjusted. Converters with independent excitation of oscillations are described in [13, 14]. In the control system of the converter with independent excitation of oscillations, it is necessary to provide for such characteristics of the conversion frequency control so that the desired valve switching conditions are observed throughout the control range [12, 15, 16]. Control characteristics are calculated for specific circuit parameters. Therefore, the parameters must be stable. The advantages of independent control are the simplicity of implementing a discrete control system and the stability of the operating frequency in the presence of a digital frequency synthesizer. The disadvantage of independent control is a significant deviation from the rated value of amplitudes and phases of oscillations with instability of circuit and load parameters, especially when working near the resonant frequency. If the load varies over a wide range – from the rated value to idling, changes in the phase shifts of oscillations in the circuit relative to the excitation voltage of the inverter u_g can lead to violations of switching conditions with an increase in power losses in the power keys of the circuit.

The self-generator excitation of oscillations present in converters such as those reported in [9, 10] occurs due to the action of positive feedback (Fig. 1, *b*) on any value – for example, on the magnitude of the current or voltage of the element of the power circuit. In control systems with self-generation, the oscillation frequency usually changes automatically with changes in the circuit parameters. However, the conditions of self-generation can be violated with deep power regulation and when the load changes. Therefore, self-generator systems are more applicable in resonant inverters with a narrow range of power control and load changes – mainly for constant load. The advantage of self-generator excitation is the automatic maintenance of the phase of oscillations in the circuit and the conditions of switching the keys with moderate instability of the circuit parameters due to the presence of positive feedback on the parameters of the oscillations. The disadvantage of self-generator excitation is the limited range of power regulation and load changes. The reason for this restriction is a possible violation of the self-generation conditions with a decrease in the amplitude of oscillations below the sensitivity thresholds of PF links, leading to a breakdown in self-generation and a failure of the output voltage.

Mixed excitation of oscillations (independent excitation with the occurrence of self-generation) (Fig. 1, *c*) avoids a possible disruption of self-generation of oscillations in the inverter circuit. At the beginning of operation, or when the conditions of self-generation are not met, the oscillations in the circuit are excited by an independent exciter generator with constant signal parameters. As the amplitude of oscillations increases to the level recorded by the detector sensor (DS), switch K switches from input 1 to input 2 and a PF self-generation begins to operate, as in [10], where self-generation is started using a thyristor. Mixed excitation should be used when introducing insensitivity zones into the elements of the PF loop to exclude false positives of elements caused by thermal noise, transient processes (which quickly end), and interference. Limiting the sensitivity of elements in the PF circuit to reduce the effects of noise and interference in turn reduces the likelihood of spontaneous self-generation. Therefore, the independent exciter creates initial oscillations with a sufficient amplitude so that when the amplitude of oscillations increases to a normal level, the PF loop reliably enters the work.

Excitation with synchronous control (Fig. 1, *d*) is realized by an independent generator, which, after establishing the rated mode of operation of the converter, begins to synchronize with free oscillations in the circuit, for example, when the circuit current passes through zero. An example of such a converter would be [11]. In this case, the frequency of oscillations becomes associated with the parameters of the resonance circuit, and switching conditions can be observed automatically with unstable parameters of the resonance circuit.

Thus, in resonant charging inverters, it is advisable to use mixed excitation systems and systems with synchronization, which make it possible to maintain the self-tuning of the inverter with an unstable inductance of the circuit.

5. 2. Comparison of ways to implement self-generation in resonant inverters

We next consider in detail the methods of implementing the self-generation of oscillations according to the schemes in Fig. 2 with phase-shifting non-resonance filters in the PF loop.

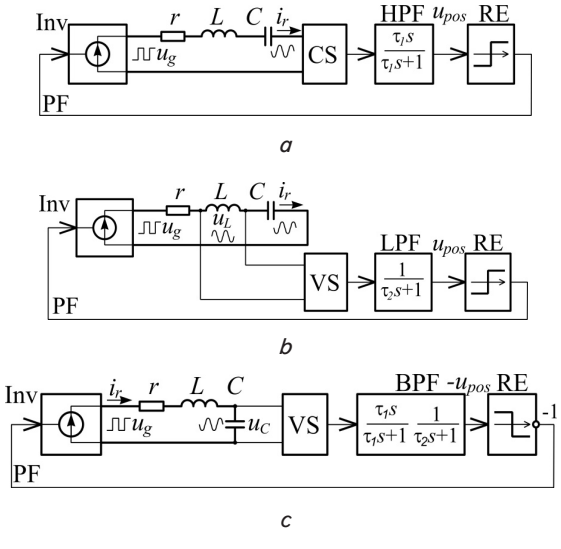

Fig. 2. Circuits of self-generating resonant inverters: *a* — with positive feedback (PF) on the current of the resonant circuit i_r and with a high pass filter (HPF); *b* — with PF by inductance voltage u_L and with a low pass filter (LPF); *c* — with PF on the voltage of capacitance u_C and with a band pass filter (BPF); Inv – Inverter, CS – Current Sensor and VS – Voltage Sensor — current and voltage sensors, RE – Relay element, u_{pos} — PF voltage

The replacement circuit of the resonant inverter is represented here by an active resonant *rLC*-circuit with a voltage source u_g. For excitation and auto-generation of oscillations, PF is used on the current of the circuit i_{pk} in Fig. 2, *a*, on the inductance voltage u_L in Fig. 2, *b*, and on the voltage on capacitance u_c in Fig. 2, *c*. Signals for PF are generated by voltage sensors DN or a DT current sensor measuring the relevant values. Practically, for obtaining PF signals in the circuits in Fig. 2, one can use the following elements: in Fig. 2, *a* – current transformer, in Fig. 2, *b* – an

additional winding of the resonant choke, and for the circuit in Fig. 2, *c* – a resistive-capacitive voltage divider. Next, signals from the quantity sensors are sent to the phase-shifting filters of low frequencies (LLF), high frequencies (HLF), or bandpass filter (BF). Filters are used to create some definite mismatch of the established frequency of self-generation ω_g relative to the resonant frequency $\omega_0 = 1/\sqrt{LC}$. This mismatch is necessary to provide key switching conditions in which switching power losses are small. From the output of the phase-shifting filters, signals are sent to relay elements P, which may have insensitivity zones or hysteresis characteristics to reduce the influence of noise and interference on the working processes in the control system. Relay elements convert signals with a shape close to a sine wave into rectangular signals that control the states of the keys of voltage inverters I. The activation of the keys corresponds to the polarity of the signals of the relay elements P in such a way that the rectangular voltages u_g generated at the output of the voltage inverters correspond to the output signals of the phase-shifting filters u_{pos}.

Applying a bandpass filter in the circuit in Fig. 2, *c* is necessary to eliminate the constant component of the PF signal by voltage on the capacitance. The constant component of the voltage on capacitance may arise due to the spread of parameters and asymmetric switching of the keys of the inverter arms. When used as a phase-shifting filter, the resulting constant component would lead to the accumulation of undesirable displacement in the PF loop and to a violation of the conditions of soft key switching. Therefore, in this case, it is necessary to use a bandpass filter with a pole frequency setting in the direction of phase delay at the operating frequency.

Thus, the phase-shifting non-resonance filters of the first and second order in the positive feedback circuit of inverters set certain shifts in the operating frequency of self-generation relative to the resonant frequency. This makes it possible to control the power of the inverter, maintaining the predefined ratio of operating frequency and resonant frequency. And with an unchanged adjustment signal, keep the specified amplitude of oscillations within acceptable limits with inductance variations.

collector-emitter or drain-source terminals for transmitting the reverse current of the transistor are used as active keys of high-frequency resonance converters. That is, in a transistor inverter when operating in the low-frequency operating frequency range (LF range), the next transistors open when currents pass through the reverse diodes of adjacent transistors. Since the diodes conducting the current must be closed by the reverse voltage, this leads to significant pulses of charge resorption currents during the restoration of the reverse impedances of the diodes. On the opening transistors during the locking of the diodes, such a large pulsed power of heat loss is released, which can disable the transistors and lead to a converter failure. Therefore, operation in the LF range of the operating frequency (Fig. 3, *a*) in a resonant converter with a transistor inverter is unacceptable.

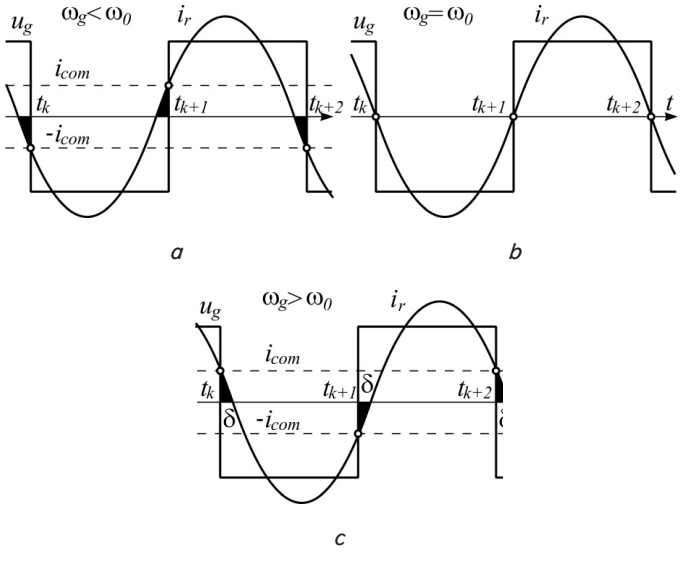

Fig. 3. Plots of inverter voltage and circuit current, explaining the switching conditions of the inverter keys: u_g – inverter voltage, i_{pk} – resonant circuit current, i_{kom} – circuit current at switching moments t_k, t_{k+1}, t_{k+2}: *a* – at LF operating frequency range ($\omega_g<\omega_0$); *b* – when operating at the resonant frequency ($\omega_g=\omega_0$); *c* – at HF operating frequency range ($\omega_g>\omega_0$)

5. 3. Key switching conditions

The switching conditions of the inverter keys are determined by the ratio of the operating frequency and the resonant frequency of the circuit. When operating at a resonant frequency $\omega_g=\omega_0$ (Fig. 3, *b*), the phase of the rectangular voltage of the inverter u_g coincides with the current phase of the circuit i_{pk}. At the moments of switching the inverter keys, when the voltage u_g is gradually changing, the alternating current i_{pk} will pass through zero. Thus, the keys of the inverter will switch at a current close to zero. Possible switching power losses will be minimal and due mainly to recharging of parasitic key and mounting capacitance [12, 15, 16].

If, as a result of the instability of the circuit parameters, the resonant frequency shifts slightly upwards, the operating frequency will be lower than the resonant frequency $\omega_g<\omega_0$ and the current of the circuit i_{pk} will outpace the voltage of the inverter u_g in phase (Fig. 3, *a*). Switching of keys at times t_k, t_{k+1}, t_{k+2} will occur at a non-zero current i_{pk}, which has already changed sign in relation to the normal direction of the current through the keys. Basically, bipolar and field-effect transistors with connected power diodes between the

When the resonant frequency of the circuit shifts downwards spontaneously, the operating frequency becomes higher than the resonant frequency $\omega_g>\omega_0$ and the current of the circuit i_{pk} begins to lag in phase from the voltage of the inverter u_g (Fig. 3, *c*). The converter operates in the HF range of the operating frequency. Switching of the keys at times t_k, t_{k+1}, t_{k+2} will occur at a non-zero current i_{pk}, which still corresponds to the normal direction of the current through the keys. Therefore, the transistors of the inverter will close at a non-zero current value. Further, the opening adjacent transistors will pass this current through themselves without a pulsed increase in the current in the switching intervals, as was observed when locking the reverse diodes. Then the converter works in the LF range of the operating frequency. Consequently, although switching losses will occur, they will be much lower than switching losses under hard switching. Therefore, the switching conditions during the operation of the resonant inverter in the HF range of the operating frequency can be considered quite acceptable.

In addition, a small margin in the operating frequency relative to the resonant frequency creates a reserve in the phase δ in Fig. 3, *c*. Phase reserve contributes to the preservation of soft switching with slight variations in circuit parameters caused by the temperature and aging of the elements of the power part of the inverter.

Thus, when determining the frequency of self-generation of oscillations, it is necessary to take into consideration that for the successful functioning of the resonant converter, it is necessary that its operating frequency should be not lower than the resonant frequency.

5. 4. Defining conditions for the self-generation of oscillations, and dependences of the frequency of self-generation

Conditions for self-generation of oscillations in the circuits of resonant inverters are created with the help of PF and can be formally represented as conditions for the instability of a closed system with a structure in Fig. 2, 3. For linearized dynamical systems, algebraic stability criteria (e. g., Ruth-Hurwitz [16]) are used, on the basis of which, in this case, it is necessary to ensure the instability of the converter system with PF. According to Lyapunov's criteria, an unstable system must have positive real parts of at least one of the roots of the characteristic equation. However, the expressions of the roots of the characteristic equation of order greater than two in general form will be cumbersome. In accordance with Hurwitz's criteria, for the instability of the system and the emergence of self-generation, it is enough to have at least one negative coefficient of the characteristic equation [16]. They were used to find the conditions for self-generation.

When exciting oscillations (when fluctuations of current and circuit voltages still have small amplitudes), circuits in Fig. 2 may be linearized. To this end, the relay element P and the inverter I are replaced by linear gearing links with finite gains, the total coefficient of which is denoted as K_{pos}. The expressions of the coefficients of the characteristic equation of the closed linearized dynamical system of the resonant inverter have been obtained. The general expression of the transfer function of an open inverter system can be written as a product. The transfer function of the resonance circuit $H_{pk}(s)$, which is defined as the ratio of the output image to the inverter voltage image, is multiplied by the transfer function of the phase-shifting filter $H_f(s)$ and by the gain factor K_{pos} of the linear inertia-free PF links. (Hereinafter $s=j\omega+\sigma$ is the Laplace operator.)

$$H_{res}(s)=H_{pk}(s)\cdot H_f(s)\cdot K_{pos}, \tag{1}$$

General characteristic equation of a PF loop-closed linearized inverter system for circuits in Fig. 2 will take the form

$$1-H_{res}(s)=0. \tag{2}$$

The specific expressions of the coefficients of equation (2) will be different for the three schemes in Fig. 2:

1) for the circuit with PF on the circuit current and with the VHF in Fig. 2, *a*, we have the following transfer function of the resonant circuit

$$H_{pk}(s)=\frac{i_{pk}(s)}{u_g(s)}=\frac{s/(\omega_0\rho)}{s^2/\omega_0^2+s/(Q\omega_0)+1}, \tag{3}$$

where $\omega_0=1/\sqrt{LC}$ is the resonant frequency of the circuit, $\rho=\sqrt{L/C}$ is the wave impedance, $Q=\rho/r$ is the Q factor of the circuit, r, L, C is the active impedance, inductance, and capacitance of the circuit. the HHF transfer function is $H_{hpf}=\tau_f s/(\tau_f s+1)$. The characteristic equation, according to (2), takes the form

$$\frac{\tau_f}{\omega_0^2}s^3+\left[\frac{\tau_f}{Q\omega_0}+\frac{1}{\omega_0^2}-\frac{K_{pos}\tau_f}{\rho\omega_0}\right]s^2+\left[\tau_f+\frac{1}{Q\omega_0}\right]s+1=0.$$

It gives the condition of instability, namely the condition of self-generation of oscillations in the form

$$\frac{\tau_f}{Q\omega_0}+\frac{1}{\omega_0}-\frac{K_{pos}\tau_f}{\rho\omega_0}<0,$$

from where we find the expression for the required gain factor in the PF loop

$$K_{pos}>r+L/\tau_f; \tag{4}$$

2) for a circuit with PF on inductance voltage and with LFF in Fig. 2, *b*, we have the following transfer function of the resonance circuit

$$H_{pkL}(s)=u_L(s)/u_g(s)=H_{pk}(s)\cdot s\cdot L. \tag{5}$$

The LFF transfer function is $H_{lpf}=1/(\tau_f s+1)$. The characteristic equation (2) takes the form

$$\frac{\tau_f}{\omega_0^2}s^3+\left[\frac{\tau_f}{Q\omega_0}+\frac{1}{\omega_0^2}-\frac{K_{pos}L}{\rho\omega_0}\right]s^2+\left[\tau_f+\frac{1}{Q\omega_0}\right]s+1=0.$$

The condition of auto-generation of oscillations

$$\frac{\tau_\phi}{Q\omega_0}+\frac{1}{\omega_0^2}-\frac{K_{pos}L}{\rho\omega_0}<0,$$

from where we find the expression for the required gain factor in the PF loop

$$K_{pos}>r\tau_f/L+1; \tag{6}$$

3) for a circuit with PF on capacitance voltage and with a bandpass filter (PF) in Fig. 2, *c*, we have the following transfer function of the resonance circuit

$$H_{pkC}(s)=u_C(s)/u_g(s)=H_{pk}(s)/(s\cdot C). \tag{7}$$

The bandwidth filter transfer function is

$H_{bpf}=\tau_1 s/((\tau_1 s+1)\ (\tau_2 s+1))$,

where τ_1 and τ_2 are the time constants of the bandpass filter (PF) links.

The characteristic equation of the PF-closed inverter system (2), in this case, takes the form

$$\frac{\tau_1\tau_2}{\omega_0^2}s^4+\left[\left(\frac{\tau_1}{Q\omega_0}+\frac{1}{\omega_0^2}\right)\tau_2+\frac{\tau_1}{\omega_0^2}\right]s^3+$$
$$+\left[\left(\tau_1+\frac{1}{Q\omega_0}\right)\tau_2+\frac{\tau_1}{Q\omega_0}+\frac{1}{\omega_0^2}\right]s^2+$$
$$+\left[\tau_1+\tau_2+\frac{1}{Q\omega_0}-K_{pos}\tau_1\right]s+1=0.$$

The condition of auto-generation of oscillations $\tau_1+\tau_2+\frac{1}{Q\omega_0}-K_{pos}\tau_1<0$, from where we find the expression for the required gain factor in the PF loop

$$K_{pos}>rC/\tau_1+\tau_2/\tau_1+1. \quad (8)$$

The values of the PF gain factors (4), (6), (8), necessary for self-generation, are provided by adjusting the sensitivity thresholds of the relay element P in Fig. 2. It is taken into consideration that the ideal relay element with zero sensitivity thresholds is a linear amplifier element with a gain factor tending to infinity.

Next, it is necessary to determine the steady-state frequency of self-generation ω_g and its dependence on the parameters of the phase-shifting filters. To this end, it is possible to consider the conditions of self-generation at a given frequency from the point of view of the phase and amplitude criteria for the instability of the dynamic system.

$$\sum\phi\left(j\omega_g\right)=0,\ |H_{res}(j\omega_g)|\geq 1. \quad (9)$$

These criteria mean that for an open system that generates unabated oscillations when the PF is closed, the total phase shift should be zero (phase balance). And the total gain (loop gain) should be at least one at the operating frequency of self-generation. From the first balance equation in (9), it is possible to find the frequency of self-generation ω_g and then, from the second inequality in (9) (from loop gain), it is possible to find the gain value necessary for self-generation in the PF loop. Self-generation frequency expressions of three resonant converter circuits with self-generation in Fig. 2 are defined as follows:

– for the circuit with PF on the circuit current and the VHF circuit in Fig. 2, *a*, the phase balance equation will be written as $\Phi_{hpf}+\Phi_{pk}=0$, where $\Phi_{hpf}=\text{arctg}(1/(\omega_g\tau_f))$ is the phase shift HHF, $\Phi_{pk}=\text{arctg}(Q(\omega_0/\omega_g)-Q(\omega_g/\omega_0)=-\delta$ is the phase shift between the voltage of the inverter u_g and the current of the resonant circuit i_{pk} according to the transfer function (3) for the operating frequency of self-generation ω_g. After substituting the expressions of phase shifts into the equation of phase balance and simplifications, an expression of the steady frequency of self-generation is derived

$$\omega_g=\omega_0\sqrt{1+rC/\tau_f}. \quad (10)$$

From this expression, it follows that the converter in Fig. 2, *a* always works in the HF operating frequency range $\omega_g>\omega_0$. With a decrease in the active impedance of the circuit r and an increase in the constant time of LFF τ_f, the self-generation frequency tends to the resonant frequency of the circuit.

For a circuit with PF on inductance voltage and with LFF in Fig. 2, *b*, a phase balance equation, according to Fig. 4, will be written as $\pi/2+\Phi_{lpf}+\Phi_{pk}$. In this expression, the angle $\pi/2$ takes into consideration the phase advance of the inductance voltage relative to the circuit current, $\Phi_{lpf}=\text{arctg}(-\omega_g\tau_f)$ is the LFF phase shift, Φ_{pk} is the phase shift between the voltage of the inverter u_g and the current of the circuit i_{pk}. The output voltages of the phase-shifting filters u_{pos_lpf} and u_{pos_hpf} in Fig. 4 correspond in phase to the output voltage of the inverter u_g for the LF and HF operating frequency ranges.

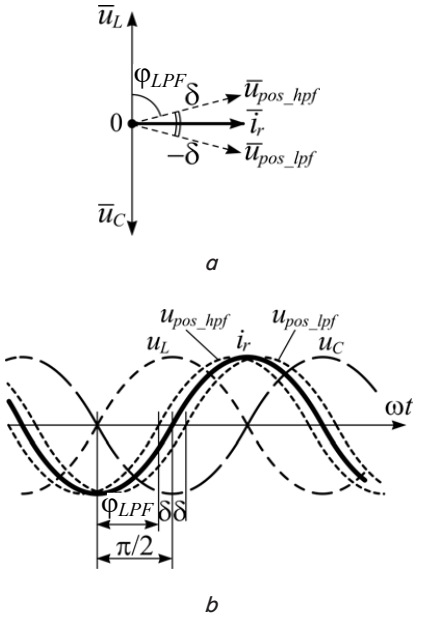

Fig. 4. Diagrams of phase displacements between oscillatory quantities in the dynamic system of a resonant inverter: *a* – phase; *b* – temporal (u_{pos_lpf}, u_{pos_hpf} – voltages at the output of phase-shifting filters for low frequencies and for high frequencies of operating frequency ranges, setting the voltage phase of the inverter u_g)

After substitutions, taking into consideration the ratio of $\pi/2+\text{arctg}(a/b)=-\text{arctg}(b/a)$, we obtain an expression of the self-generation frequency $\omega_g=\omega_0\sqrt{1+rC/\tau_f}$, which coincides with the previously obtained expression (10) for PF on the current of the circuit. The self-generation frequency is also in the HF operating frequency range.

For the scheme with PF on capacitance voltage and with a pass filter (PF) in Fig. 2, *c*, the phase balance equation, according to Fig. 4, will be recorded as $\pi/2+\Phi_{bpf}+\Phi_{pk}=0$, where the angle $\pi/2$ takes into consideration the phase advance of the inverted (shifted by 180°) voltage on capacitance, relative to the circuit current, $\phi_{\text{пф}}=\text{arctg}\left(\left(1-\tau_1\tau_2\omega_g^2\right)/\left(\omega_g\left(\tau_1+\tau_2\right)\right)\right)$ is the phase shift of PF, Φ_{pk} is the phase shift between the voltage of the inverter u_g and the current of the circuit i_{pk}. After substitutions, taking into consideration the ratio $\pi/2+\text{arctg}(a/b)=-\text{arctg}(b/a)$, we obtain an expression for the self-generation frequency

$$\omega_g=\frac{1}{\tau\sqrt{2Q}}\times$$
$$\times\sqrt{2\tau\omega_0+Q\omega_0^2\tau^2+Q+\sqrt{\begin{matrix}(2\tau\omega_0)^2+4\tau^3\omega_0Q+4\tau\omega_0Q+\\+\tau^4\omega_0^4Q^2-2\left(\tau\omega_0Q\right)^2+Q^2\end{matrix}}}, \quad (11)$$

where $\tau_1=\tau_2=\tau$ are PF time constants equal to each other. The expression of the self-generation frequency for the various time constants τ_1 and τ_2 is also built but is not given here because of its bulkiness. The frequency of self-generation in this case is also in the RF range of the operating frequency. Owing to the phase-shifting filters in the circuits in Fig. 2, it reliably provides reserves for phase δ – the phase advance of the inverter voltage relative to current fluctuations, maintaining the frequency of self-generation above the resonant frequency of the circuit.

For the converter to work in the LF range of the operating frequency, it is advisable to use PF on the circuit current with a slight delay in phase. In the circuit in Fig. 2, *a*, LFF should be inserted instead of HFF. Then the balance of phases will be recorded, according to Fig. 4, *a*, as $\Phi_{lpf}+\Phi_{pk}=0$. After substituting the above-recorded expressions Φ_{lpf} and $\Phi_{pk}=-\delta$, the expression of the steady-state self-generation frequency for the LF of the operating frequency range is obtained

$$\omega_g = \omega_0\sqrt{1/\left(1+r\tau_f/L\right)}, \qquad (12)$$

from which it is not difficult to see that $\omega_g<\omega_0$. The operation of the resonance converter in the LF range of the operating frequency can be justified (and necessary) when used as keys of the thyristor inverter. Thyristors will lock at the intervals of reverse current (darkened areas in Fig. 3, *a*). At the same time, the current surges on the opening thyristors when the charge carriers of the closing adjacent diodes are absorbed will not be so great since the recovery time of the reverse impedance of the diode is comparable to the time of unlocking the thyristor.

Phase characteristics shown in Fig. 5 demonstrate changes in the frequency of self-generation when the phase-shifting filter constants change. Curves 2–4 correspond to the inverted phase characteristics of LFF in the PF current converter with the abscissa axis. Curves 5–7 correspond to the inverted phase characteristics of the HFF axis in the PF-overcurrent converter in Fig. 2, *a*. They also correspond to the inverted relative to the abscissa axis and shifted down by 90° the phase characteristics of LFF in the converter with PF voltage at inductance in Fig. 2, *b*. The intersection points of all these curves with the phase characteristic of the circuit (curve 1) determine the established frequencies of self-generation. For curves 2–4, the self-generation frequencies are always less than the resonant frequency of the circuit. The converter with PF for current and LFF always operates in the LF range of the operating frequency ($\omega_g<\omega_0$). For curves 5–7, the self-generation frequencies are always higher than the resonant frequency of the circuit. Converters with PF for current and HFF, and with PF for voltage inductance and LFF, always operate in the HF range of the operating frequency ($\omega_g>\omega_0$).

In Fig. 5, we marked frequencies $\omega^*_{g1LF}<\omega^*_{g2LF}$, which correspond to the time constants of LFF $\tau_f=10/\omega_0$ and $\tau_f=1/\omega_0$. The frequencies $\omega^*_{g1HF}<\omega^*_{g2HF}$ correspond to the filter time constants $\tau_f=10/\omega_0$ and $\tau_f=1/\omega_0$. It follows that in the LF range of the operating frequency, with an increase in the constant of LFF, the frequency of self-generation decreases and moves away from the resonant frequency of the circuit. In the HF range, an increase in the time constant of the phase-shifting filters also leads to a decrease in the frequency of self-generation and its approximation to the resonant frequency of the circuit.

For the circuit in Fig. 2, *c*, with a voltage PF on capacitance at large band filter time constants $\tau_1>1/\omega_0$ and $\tau_2>1/\omega_0$, the phase balance with an acceptable approximation is illustrated by curves 1 and 5–7 in Fig. 5.

As discussed above, the circuits in Fig. 2 provide self-generation only in the HF range of the operating frequency. If you replace HFF with LFF in the circuit in Fig. 2, *a*, you can go to the LF range of the operating frequency and stay in it. When designing powerful resonant generators of harmonic oscillations, the characteristics of the circuit with the ability to adjust the self-generation frequency within both the LF and HF conversion frequency ranges are of particular interest. According to Fig. 4, the phase-shifting filter must provide a negative or positive phase shift $\pm\delta$ relative to the oscillations of the resonant current during its tuning. These requirements are met by a bandpass filter or an active phase filter with zero phase shift at the center frequency. Consider the circuit in Fig. 2, *a* with PF on the current, in which, instead of HFF, we shall use the bandpass filter from the circuit in Fig. 2, *c* having a symmetric phase characteristic $\phi_{pf}=\operatorname{arctg}\left(\left(1-\tau_1\tau_2\omega_g^2\right)/\left(\omega_g\left(\tau_1+\tau_2\right)\right)\right)$. The phase balance will take the form $\Phi_{bpf}+\Phi_{pk}=0$. The frequency of self-generation will be determined by the ratio

$$\omega_g = \omega_0\sqrt{\frac{Q\omega_0\left(\tau_1+\tau_2\right)+1}{\tau_1\tau_2\omega_0^2+Q\omega_0\left(\tau_1+\tau_2\right)}}. \qquad (13)$$

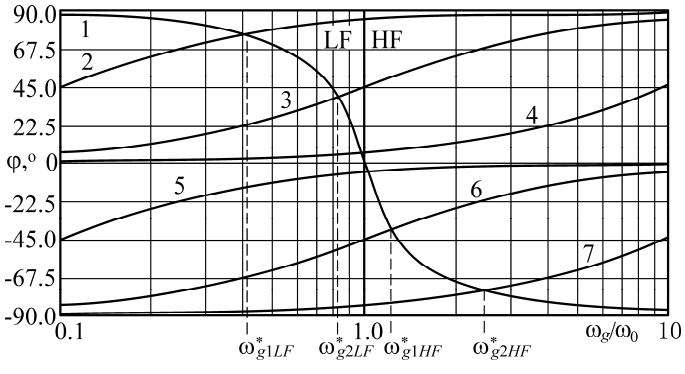

Fig. 5. Phase characteristics of the resonant circuit (curve 1) combined with the phase characteristics of the first-order phase-shifting filters (curves 2–7) for different filter time constants: 2 and 5 – for $\tau_f=10/\omega_0$, 3 and 6 – for $\tau_f=1/\omega_0$, 4 and 7 – for $\tau_f=0.1/\omega_0$

The self-generation frequency ω_g in (12) may be less and greater than the resonant frequency ω_0 depending on the values of the time constants τ_1 and τ_2.

To visualize the degree of influence of the settings of phase-shifting filters in the PF loop of resonant converters on the frequency of self-generation, the dependences of the frequency of self-generation ω_g on the frequencies were calculated. The pole settings of the phase-shifting filters are defined as $\omega_{pol}=1/\tau_f$, where τ_f is the first-order filter time constant, $\tau_1=\tau_f\sqrt{k_{bw}}$ and $\tau_2=\tau_f/\sqrt{k_{bw}}$ are the time constants of the bandpass filter links, $k_{bw}\geq1$ is the bandwidth coefficient of the bandwidth filter. Figure 6 shows the plots of these dependences. Plot 1 is calculated from (11), plot 2 – (10), plots 3–5 – (13), plot 6 – (12) for wave impedance $\rho=1$ and Q factor $Q=2$, which roughly corresponds to actual converters.

The gain factors required for the emergence and maintenance of self-generation in the converter PF loop can be found from the requirement for the value of the loop gain (9), which is equal to the product of the modules of the transfer functions of the links of the PF circuit (1)

$$\left|H_{pk}\left(j\omega_g\right)\cdot H_f\left(j\omega_g\right)\right|\cdot K_{pos}\geq1,$$

hence

$$K_{pos}\geq\left|H_{pk}\left(j\omega_g\right)\cdot H_f\left(j\omega_g\right)\right|^{-1}. \qquad (14)$$

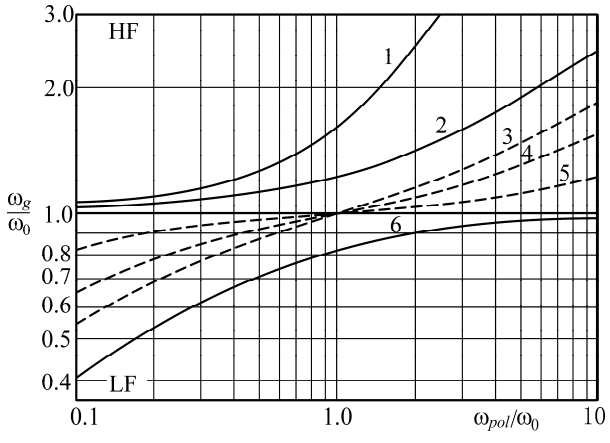

Fig. 6. Dependences of the frequency of self-generation ω_g on the frequency of the pole ω_{pol} of the phase-shifting filters relative to the resonant frequency of the circuit ω_0: 1 – for positive voltage feedback on capacitance (Fig. 2, *c*) with a bandpass filter; 2 – for positive current feedback with a high-frequency filter (Fig. 2, *a*) and for positive feedback on inductance voltage with a low-frequency filter (Fig. 2, *b*); 3, 4, 5 – for positive current feedback with a bandpass filter at different bandwidth coefficients k_{bw}=1; 10; 100, respectively; 6 – for positive current feedback with a low-pass filter

Calculated from (14), the minimum required gains in the PF loop for resonant inverters with different links in the PF are given in Table 1 at different settings of the relative frequencies of the poles of the phase-shifting filters $\omega_{pol}=1/\tau_f$.

Table 1

Gain factors K_{pos_min} in the positive feedback loop of resonant inverters

Inverter type	Frequencies of tuning phase-shifting filters ω_{pol}/ω_0				
	0.1	0.3	1.0	3.0	10
– with inductance voltage PF and LFF, HF range	5.048	1.797	0.833	0.767	0.883
– with circuit current PF and LFF, HF range	0.505	0.539	0.833	2.3	8.833
– with capacitance voltage PF and BPF*, HF range	5.325	2.146	1.614	4.111	22.277
– with circuit current PF and LFF, HF range	8.833	2.583	0.833	0.548	0.505

Note: for the bandpass filter, it is accepted that $\tau_1=\tau_2=\tau_f$

If, instead of relay elements P in PF in Fig. 2, *a–c*, we use reinforcement links, their transmission coefficients K_{pos} should take values not less than those given in Table 1. When using noise-resistant relay elements with an insensitivity zone or with a hysteresis characteristic, their sensitivity thresholds U_{th} should be selected in such a way that the self-generation condition is met

$$U_{th} < U_{s\_min} \cdot K_{sen} / K_{pos\_min}, \quad (15)$$

where U_{s_min} is the minimum supply voltage of the inverter, K_{sen} is the transmission coefficient of the current sensor (V/A) or voltage (V/V), K_{pos_min} is the value from Table 1. It is worth noting that condition (15) is easy to fulfill in real inverter circuits.

5. 5. Simulation results

To verify the accuracy of the obtained dependences of the frequency of self-generation, simulation experiments were conducted with model schemes in Fig. 7, *a–c*, which correspond to the circuits of resonant inverters in Fig. 2, *a–c*. A voltage inverter (*Inverter* elements in Fig. 7) is a two-key, reverse diode semi-bridge circuit that is powered by a bipolar voltage $\pm U_s$. Phase-shifting filters F are implemented in the form of passive *RC*-filters with transfer functions $H_{hpf}(s)=\tau_\Phi s/(\tau_\Phi s+1)$ in Fig. 7, *a*, $H_{lpf}(s)=1/(\tau_f s+1)$ in Fig. 7, *b*, and $H_{bpf}(s)=\tau_1 s/(\tau_1\tau_2 s^2+(\tau_1+\tau_{12}+\tau_2)s+1)$ in Fig. 7, *c* with time constants $\tau_f=R_\tau\cdot C_\tau$, $\tau_1=R_{\tau1}\cdot C_{\tau1}$, $\tau_{12}=R_{\tau1}\cdot C_{\tau2}$, $\tau_2=R_{\tau2}\cdot C_{\tau2}$, respectively.

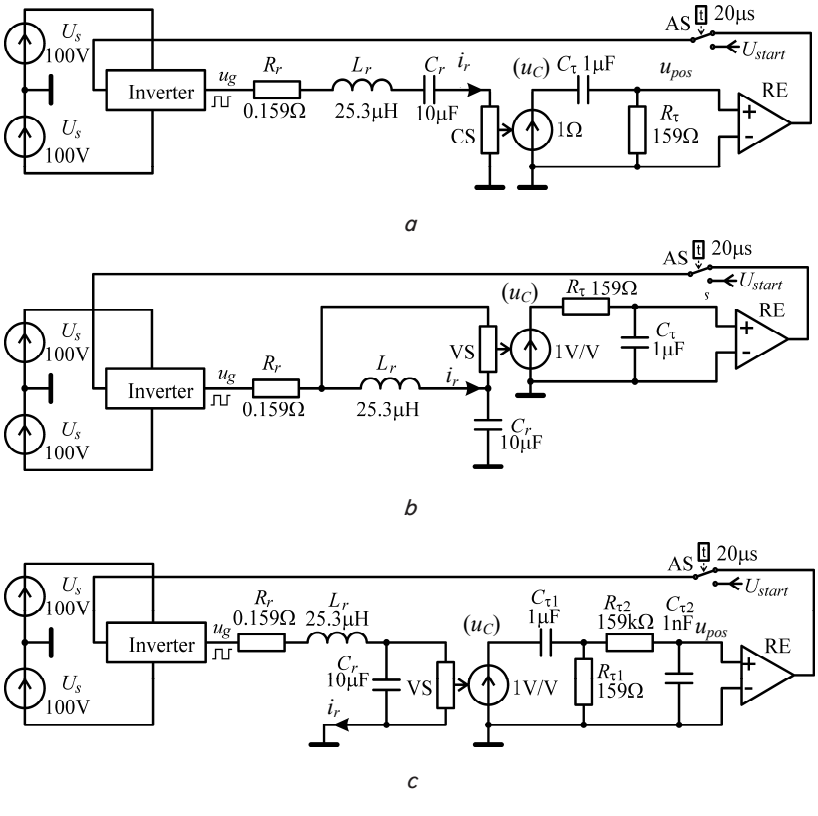

Fig. 7. Simulation models of inverters with self-generation in Fig. 2, *a–c*, respectively: U_s – power voltage; u_g – voltage of the inverter half-bridge; (i_r) – signal of the circuit current sensor; (u_L) – signal of the inductance voltage sensor; (u_C) – signal of the voltage sensor on capacitance; u_{pos} – loop voltage PF; *Inverter* – voltage inverter; AS (Auto Start) – autostart elements; Φ – phase-shifting filter; RE (Relay Element) – comparator

The parameters of the resonance circuit of inverter models are as follows: resonant frequency

$$f_0 = 1/\left(2\pi\sqrt{L_r C_r}\right) = 10000 \text{ Hz},$$

the loop Q factor $Q = \sqrt{L_r}/\left(R_r\sqrt{C_r}\right)$ (for R_r=0.795 Ohm Q=2, for R_r=0.159 Ohm Q=10), the frequency of free oscillations

$$f_1 = f_0\sqrt{1-1/\left(4Q^2\right)}$$

(for Q=2 f_1=9688 Hz, for Q=10 f_1=9993 Hz).

During model experiments, the schemes in Fig. 7, *a–c* were started with zero initial conditions at different values of the Q factor of the circuit and time constants of the phase-shifting filters. The Q factor of the circuit was changed by changing the impedance R_r. The time constants of the phase-shifting filters were changed by the impedances R_τ, $R_{\tau 1}$, $R_{\tau 2}$. In particular, different values of impedances corresponded to different relative frequencies of the poles of filters $\omega_{pol}/\omega_0 = 1/(\omega_0\tau_f)$, where $\omega_0 = 2\pi f_0 = \sqrt{1/(L_r C_r)}$ is the frequency of resonance given in Table 2.

Table 2

Filter impedance and pole frequency correspondences

Impedance value	159	79.5	53	31.8	22.7	15.9	7.95	5.3	3.18	2.27	1.59
Pole relative frequencies	0.1	0.2	0.3	0.5	0.7	1.0	2.0	3.0	5.0	7.0	10

For the bandpass filter, we accepted $\tau_1=\tau_2=\tau_f$, and τ_{12}=0,001τ_f was adopted to reduce the mutual influence of the links.

Oscillations in the circuits were excited by a 20 μs inverter control start pulse (AS keys in Fig. 7). After starting self-generation and reaching the amplitudes of fluctuations of stationary values (2–3 ms model time), the simulation stopped, and the periods of stationary self-oscillations were measured. Plots of the processes of starting current oscillations at different Q factors of the circuit are shown in Fig. 8.

Based on simulation modeling, the series of self-generation frequencies at different values of the circuit Q factor and different frequencies of the poles of the phase-shifting filters were determined, given in the form of plots in Fig. 9. There, for comparison with experimental plots, dashed lines are plots of theoretical dependences of self-generation frequencies, calculated from (10), (11).

Thus, during model experiments, it was found that the conditions of self-generation in resonant inverters with phase-shifting filters depend on the sensitivity of the relay element in the positive feedback circuit of the inverter. The operating frequency corresponds to the theoretical values more accurately, the lower the time constant of the phase-shifting filter and the higher the Q factor of the resonant circuit.

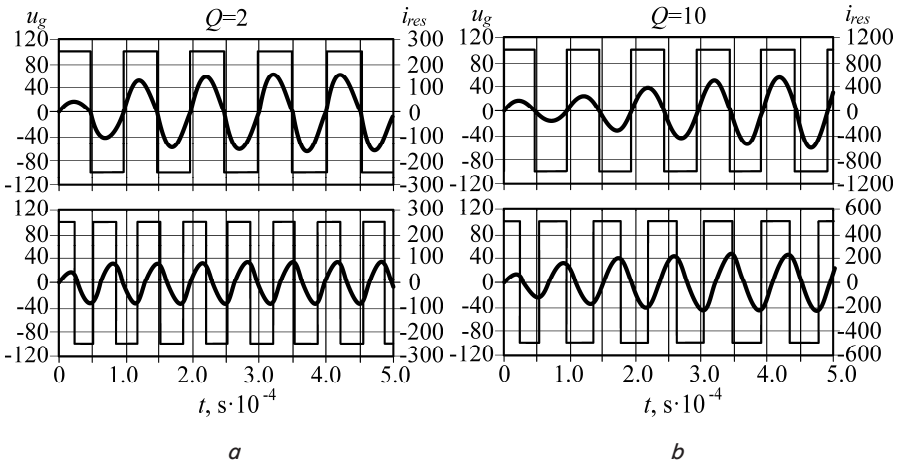

Fig. 8. Plots of the inverter half-bridge voltage and circuit current at different values of the circuit Q factor: *a* — Q=2; *b* — Q=10 (the upper plots correspond to ω_{pol}=0,1ω_0 and the operating frequency close to the resonant frequency of the circuit; the lower plots correspond to ω_{pol}=10ω_0 and higher operating frequency)

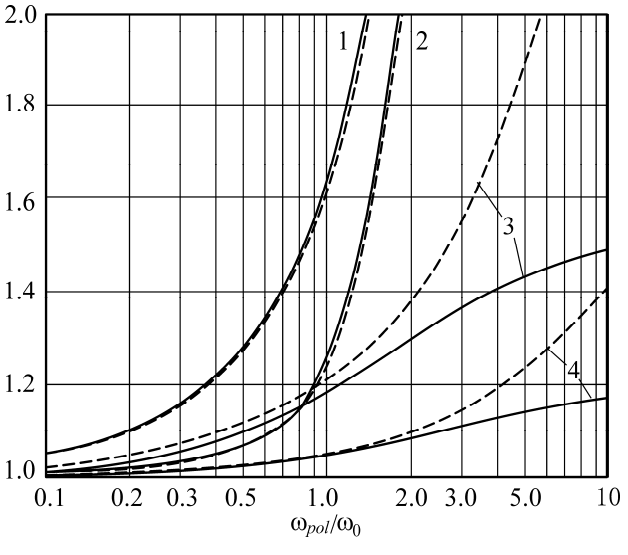

Fig. 9. Experimental dependences (solid lines) of self-generation frequencies ω_g on the frequencies of the phase-shifting filters settings ω_{poh} combined with theoretically calculated dependences (dotted lines): 1 and 2 — voltage PF on capacitance with a bandpass filter (Fig. 7, *c*) for Q=2 and for Q=10; 3 and 4 — positive feedback on the circuit current or inductance voltage with a first-order filter (Fig. 7, *a, b*) for Q=2 and for Q=10

6. Discussion of results of studying the self-generating resonant inverters and positive feedback

The results of our study are explained by the consideration of the calculated analytical dependences and their comparison with the modeling data. From Fig. 5, it follows that with an increase in the time constant of the phase-shifting filters, the operating frequency of self-generation decreases. In the LF range, the operating frequency is further away from the resonant frequency of the circuit. In the HF range, the operating frequency asymptotically approaches the resonant frequency of the circuit. However, the changing operating frequency does not cross the boundary of the

resonant frequency, which reliably sets the frequency range of the inverter with self-generation.

As can be seen from plots 2 and 6 in Fig. 6, changing the frequency of tuning phase-shifting filters in a wide range (a hundred times) changes the frequency of self-generation by 2.5 times. Thus, if the frequencies of the HF and LFF poles correspond to the resonant frequency $\omega_{pol}=\omega_0=1/\tau_f$, the calculated self-generation frequencies for the LF and HF operating frequency ranges will be $\omega_{gLF}=0.816\omega_0$, $\omega_{gHF}=1.225\omega_0$ and will differ by an equal number of times from the resonant frequency ω_0. The phase reserves between the voltage of the inverter and the circuit current will be quite large: $\delta\approx\pm 40^{\circ}$. When the Q factor of the circuit is increased to Q=10, these values will equal to $\omega_{gLF}=0.953\omega_0$, $\omega_{gHF}=1.049\omega_0$, $\delta\approx\pm 44^{\circ}$. The self-generation frequencies approached the resonant frequency, and the phase reserves became slightly higher, which can be considered an useful factor from the point of view of soft switching of the inverter keys with changes in the impedance of circuit loss.

Plots 3–5 (Fig. 6) demonstrate that when the band of the pass filter in the converter with PF on the circuit current (increase in the coefficient k_{bw}), the effect of the central frequency of the filter tuning on the self-generation frequency decreases. Therefore, if the operating frequency is to be tuned as precisely as possible to a resonant frequency or to a specific operating frequency near the resonant frequency, it is advisable to narrow the bandwidth of the filter $k_{bw}\rightarrow 1$. If the resonant circuit is characterized by instability, it is advisable to extend the bandwidth of the filter k_{bw}=10...100 to maintain self-generation conditions in a wide range of operating frequency changes.

The comparison of dependences in Fig. 6 reveals that plot 1 shows the strongest dependence of the self-generation frequency on the bandwidth filter tuning frequency but the operating frequency always remains higher than the resonant frequency.

Plots 2, 6 (Fig. 6) demonstrate changes in the operating frequency of self-generation only in the HF and only in the LF bands at any frequencies of tuning the first-order phase-shifting filters. That makes it possible to implement phase-frequency regulation by changing the time constant of the phase-shifting filters without violating the switching conditions of the inverter keys. Plots 3–5 (Fig. 6) correspond to an inverter with a bandpass filter in the PF current circuit, which implements the adjustment of the operating frequency on both sides near the resonant frequency in the LF and HF bands. The steepness of the frequency regulation will be the greater the narrower the bandwidth in the PF circuit. Tuning the operating frequency below and above the resonant frequency of the circuit can be useful in special induction communication systems. In this case, the keys of the inverters must allow switching at forward and reverse current.

Next, the modeling data are discussed. Distortions of the sinusoidal form of oscillations with an increase in the operating frequency and with a decrease in Q factor are visible from comparisons of the shape of the oscillations in Fig. 8, *a, b*. At an operating frequency close to the resonant frequency, the shape of the current oscillations differs little from the sinusoid, and with an increase in the operating frequency, the current shape becomes closer to the triangular shape. The shape of the oscillations is also significantly distorted with a decrease in the Q factor of the circuit. When the circuit becomes similar to an aperiodic link, the shape of the oscillations approaches exponential waves. However, the above theoretical data (10) to (13) were obtained for the first harmonics of oscillations. That is, they are valid for the sinusoidal shape and can allow for errors when deviating the shape of the inverter voltage from the sine wave. Therefore, theoretical dependences were also tested by simulation and for the sinusoidal voltage of the inverters u_g in the circuits in Fig. 7, *a–c*. That is, they are valid for the sinusoidal shape and can allows for errors in deviating the shape of the inverter voltage from the sine wave. Therefore, theoretical dependences were also tested using model experiments and for the sinusoidal voltages of inverters in the circuits in Fig. 7, *a–c*. At the same time, the simulation data converged with theoretical data with an accuracy of no less than 5 % in the frequency range from 0.1 to 10 relative to the resonant frequency of the circuit.

As can be seen from the plots in Fig. 9, the dependences of self-generation frequencies for the circuit with PF on voltage on capacitance and with a bandpass filter in Fig. 7, *c*, obtained as a result of simulation modeling, practically coincide with theoretical dependences. For schemes with the first-order filters in Fig. 2, *a, b*, the experimental dependences (obtained from simulation modeling) begin to differ significantly from theoretical ones (pairs of plots 3, 4) with a decrease in the time constant of filters (an increase in the frequency of the pole ω_{pol}). The discrepancy between the experimental and theoretical plots increases with an increase in the operating frequency and with a decrease in the Q factor of the circuit, which is explained by distortions of the sinusoidal form of oscillations. Since the voltage shape of the inverter half-bridge is rectangular, the lower the Q factor of the circuit, the greater the proportion of harmonics present in the fluctuations of current and voltage on the capacitance of the circuit.

On the other hand, deviations from the sinusoidal shape of oscillations introduce additional phase shifts in the phase-shifting filters. The phase shifts of the first-order filters were more sensitive to distortions of the sinusoidal waveform than the phase shift of the bandpass filter. Therefore, in the scheme with a band phase-shifting filter in Fig. 7, *c*, depending on the frequencies of self-generation obtained as a result of simulation modeling, differ little from the theoretically calculated dependences. The resulting dependences in Fig. 9 are recommended for use when the values of the Q factor of the circuit are within Q=2...10. The established theoretical dependences of the operating frequency (10) to (13) have an acceptable accuracy for engineering calculations for Q=5 or more Q factors. For a more accurate theoretical determination of the dependences of self-generation frequencies at low Q factor of the circuit (Q<5), it is advisable to use the method of superimposing the components of the circuit current [17], applicable for studying the parameters of stationary processes in the resonant inverter circuit.

The results at this stage of our study were obtained for the equivalent circuit of the primary side of the charger – a sequential resonance inverter with self-generation. The advancement of this study is the implementation of self-generation based on signals from the secondary side (from the receiving inductor) of the charger. That would make

it possible to self-adjust the charging inverter, taking into consideration the coupling coefficient between the inductors and the output current, and thus improve the dynamics of the charging system under mechanical disturbances. However, there are difficulties in mathematical modeling of a non-stationary resonance system, which are planned to be overcome by combining numerical and theoretical analysis of the system.

7. Conclusions

1. Of the considered methods of excitation of oscillations in charge resonant inverters, it is advisable to use mixed (independent and self-generator) excitation of oscillations or excitation with subsequent synchronization. This would increase the stability of the system to interference under a standby mode and implement auto-tuning of the system to the parameters of the circuit under an operating mode.

2. From the point of view of noise immunity in the positive feedback loop of inverters, it is advisable to use low-frequency filters or bandpass filters. Therefore, for operation in the LF range of the operating frequency, positive feedback on the circuit current is preferred. For the HF range, positive feedback on inductance voltage and capacitance voltage is preferred.

3. To ensure optimal conditions for switching transistors, the circuit current should δ=+0...90° lag in phase from the voltage of the inverter. Therefore, the operating frequency should be higher than the resonant frequency, which is provided by the proposed schemes of inverters with phase-shifting non-resonant filters in the PF loop when changing the time constant of the filters over wide limits.

4. The thresholds of sensitivity of relay elements in schemes with phase-shifting non-resonance filters in the PF loop have been defined. Exact values are determined experimentally or based on simulation modeling. An excessive increase in the sensitivity of these elements causes an undesirable reaction of the system to electromagnetic interference. Reducing the sensitivity will lead to the attenuation of self-generation. When the first-order filters are used in positive feedback, the operating frequency ranges of the inverters do not cross the resonant frequency. When using bandpass filters of the second (and larger) orders, the operating frequency can be rearranged below and above the resonant frequency.

5. The operating frequency of the inverter corresponds to the theoretically calculated values the more accurately, the lower the time constant of the phase-shifting filter and the higher the Q factor of the circuit. The proposed theoretical dependences of the operating frequency have an acceptable accuracy for engineering calculations for Q=5 or more. The obtained dependences of self-generation frequencies on the frequencies of the phase-shifting filters settings are recommended for use at the values of the circuit Q factor within Q=2...10.

References

1. Guidi, G., Suul, J. A., Jenset, F., Sorfonn, I. (2017). Wireless Charging for Ships: High-Power Inductive Charging for Battery Electric and Plug-In Hybrid Vessels. IEEE Electrification Magazine, 5 (3), 22–32. doi: https://doi.org/10.1109/mele.2017.2718829
2. Karimi, S., Zadeh, M., Suul, J. A. (2020). Evaluation of Energy Transfer Efficiency for Shore-to-Ship Fast Charging Systems. 2020 IEEE 29th International Symposium on Industrial Electronics (ISIE). doi: https://doi.org/10.1109/isie45063.2020.9152219
3. Abou Houran, M., Yang, X., Chen, W. (2018). Magnetically Coupled Resonance WPT: Review of Compensation Topologies, Resonator Structures with Misalignment, and EMI Diagnostics. Electronics, 7 (11), 296. doi: https://doi.org/10.3390/electronics7110296
4. Yeon, J.-E., Cho, K.-M., Kim, H.-J. (2015). A 3.6kW single-ended resonant inverter for induction heating applications. 2015 17th European Conference on Power Electronics and Applications (EPE'15 ECCE-Europe). doi: https://doi.org/10.1109/epe.2015.7309110
5. Kumar, A., Sadhu, P. K., Raman, R., Singh, J. (2018). Design Analysis of Full-Bridge Parallel Resonant Inverter for Induction Heating Application Using Pulse Density Modulation Technique. 2018 International Conference on Power Energy, Environment and Intelligent Control (PEEIC). doi: https://doi.org/10.1109/peeic.2018.8665571
6. UCC25600 8-Pin High-Performance Resonant Mode Controller (2015). Texas Instruments Incorporated. Available at: https://www.ti.com/lit/ds/symlink/ucc25600.pdf?ts=1639351167815
7. Lin, B.-R. (2021). Implementation of a Resonant Converter with Topology Morphing to Achieve Bidirectional Power Flow. Energies, 14 (16), 5186. doi: https://doi.org/10.3390/en14165186
8. Bose, B. K. (2013). Modern Power Electronics and AC Drives. PHI Learning Pvt Ltd.
9. Xu, L., Ke, G., Chen, Q., Ren, X., Zhang, Z. (2020). A Self-Oscillating Resonant Converter with Precise Output Voltage Control. 2020 IEEE 9th International Power Electronics and Motion Control Conference (IPEMC2020-ECCE Asia). doi: https://doi.org/10.1109/ipemc-ecceasia48364.2020.9367684
10. Cortes-Rodriguez, J.-A., Ponce-Silva, M. (2012). Self-Oscillating DC-DC Resonant Converter. 2012 IEEE Ninth Electronics, Robotics and Automotive Mechanics Conference. doi: https://doi.org/10.1109/cerma.2012.56
11. Pavlov, G., Pokrovskiy, M., Vinnichenko, I. (2018). Load Characteristics of the Serial-to-serial Resonant Converter with Pulse-number Regulation for Contactless Inductive Energy Transfer. 2018 IEEE 3rd International Conference on Intelligent Energy and Power Systems (IEPS). doi: https://doi.org/10.1109/ieps.2018.8559590

12. Engelkemeir, F., Gattozzi, A., Hallock, G., Hebner, R. (2019). An improved topology for high power soft-switched power converters. International Journal of Electrical Power & Energy Systems, 104, 575–582. doi: https://doi.org/10.1016/j.ijepes.2018.07.049
13. Pavlov, G. V., Vinnichenko, I. L., Obrubov, A. V. (2016). Frequency converter with the reduced thd of the output voltage. Tekhnichna Elektrodynamika, 2016 (5), 14–16. doi: https://doi.org/10.15407/techned2016.05.014
14. Vinnychenko, D., Nazarova, N. (2018). Power Converter Adaptive Control System of the Installation for Production of Nanocarbons from Gaseous Hydrocarbons. 2018 IEEE 38th International Conference on Electronics and Nanotechnology (ELNANO). doi: https://doi.org/10.1109/elnano.2018.8477539
15. Resonant circuits and soft switching (LLC resonant converter and resonant inverter) (2019). Resonant circuits and soft switching application note. Toshiba Electronic Devices & Storage Corporation. Available at: https://www.google.com/url?sa=t&rct=j&q=&esrc=s&source=web&cd=&ved=2ahUKEwiU7Ybn-OD0AhXL57sIHTSpAoEQFnoECAQQAQ&url=https%3A%2F%2Ftoshiba.semicon-storage.com%2Finfo%2Fdocget.jsp%3Fdid%3D68571&usg=AOvVaw2pv3oJiH9wee6qVlQZYdSc
16. Nakra, B., Singh, S. (2017). Theory and Applications of Automatic Controls. New Age International (P) Ltd Publishers, 376.
17. Pavlov, G., Obrubov, A., Vinnychenko, I. (2021). Design Procedure of Static Characteristics of the Resonant Converters. 2021 IEEE 3rd Ukraine Conference on Electrical and Computer Engineering (UKRCON). doi: https://doi.org/10.1109/ukrcon53503.2021.9575698